Acute pharmacodynamic and antivascular effects of the vascular endothelial growth factor signaling inhibitor AZD2171 in Calu-6 human lung tumor xenografts

Neil R. Smith,[1] Neil H. James,[1] Ian Oakley,[1] Anna Wainwright,[1] Clive Copley,[2] Jane Kendrew,[1] Lynsey M. Womersley,[1] Juliane M. Jürgensmeier,[1] Stephen R. Wedge,[1] and Simon T. Barry[1]

[1]Cancer Bioscience, AstraZeneca, and [2]Antibodies and Imaging, Discovery Enabling Capabilities and Science, Alderley Park, Macclesfield, Cheshire, United Kingdom

Abstract

The vascular endothelial growth factor-A (VEGF-A) signaling pathway, a key stimulant of solid tumor vascularization, is primarily dependent on the activation of the endothelial cell surface receptor VEGF receptor-2 (VEGFR-2). AZD2171 is an oral, highly potent small-molecule inhibitor of VEGFR tyrosine kinase activity that inhibits angiogenesis and the growth of human tumor xenografts *in vivo*. Here, we show pharmacodynamic changes in VEGFR-2 phosphorylation induced by AZD2171. In mouse lung tissue, a single dose of AZD2171 at 6 mg/kg inhibited VEGF-A–stimulated VEGFR-2 phosphorylation by 87% at 2 h with significant inhibition (≥60%) maintained to 24 h. To examine inhibition of VEGFR-2 phosphorylation in tumor vasculature by immunohistochemistry, a comprehensive assessment of antibodies to various phosphorylation sites on the receptor was undertaken. Antibodies to the phosphotyrosine epitopes pY1175/1173 and pY1214/1212 were found suitable for this application. Calu-6 human lung tumor xenografts, from mice receiving AZD2171 or vehicle treatment (p.o., once daily), were examined by immunohistochemistry. A significant reduction in tumor vessel staining of phosphorylated VEGFR-2 (pVEGFR-2) was evident within 28 h of AZD2171 treatment (6 mg/kg). This effect preceded a significant reduction in tumor microvessel density, which was detectable following 52 h of AZD2171 treatment. These data show that AZD2171 is a potent inhibitor of VEGFR-2 activation *in vivo* and suggest that AZD2171 delivers therapeutic benefit in Calu-6 tumors by targeting vessels dependent on VEGFR-2 signaling for survival. In addition, this work highlights the utility of measuring either pY1175/1173 or pY1214/1212 on VEGFR-2 as a pharmacodynamic marker of VEGFR-2 activation. [Mol Cancer Ther 2007;6(8):2198–208]

Introduction

Vascular endothelial growth factor-A (VEGF-A) plays a critical role in inducing vascular growth and remodeling during development and in a number of pathologic conditions including the angiogenesis required to support solid tumor growth (1). VEGF-A signaling is predominantly mediated through the activation of VEGF receptor-2 (VEGFR-2; KDR/flk-1), which can stimulate endothelial cell proliferation, migration, vascular permeability, and neovascular survival (reviewed in ref. 2). That inhibition of VEGF-A signaling can provide benefit in the clinical treatment of cancer has been shown by the VEGF-A neutralizing antibody bevacizumab (Avastin, Genentech/Roche) when used in combination with cytotoxic chemotherapy (3).

In addition to bevacizumab, other approaches to inhibit VEGF signaling are under investigation, including alternative ways of sequestering VEGF-A (4), preventing ligand binding to VEGFR-2 (5) or using small-molecule VEGFR tyrosine kinase inhibitors such as AZD2171 (6) or AG013736 (4). These approaches give profound effects preclinically, reducing tumor growth and tumor microvessel density (MVD) significantly upon chronic treatment. Until recently, little was known about the acute effects of a VEGF signaling inhibitor in normal and tumor vasculature. Detailed studies in a range of model systems have now shown that certain vessels are highly sensitive to VEGF signaling (4, 5, 7, 8). Assessment of the early effects of VEGF signaling inhibition on the vasculature of pancreatic islet tumors in RIP-Tag2 transgenic mice showed that both VEGF-Trap and the VEGFR-2 inhibitor AG013736 can reduce the MVD as early as 24 h after the first dose of inhibitor, with more profound reductions in MVD at later time points (4). Examining the temporal effects of these agents on tumor vasculature has therefore challenged the view that inhibiting VEGF signaling merely prevents growth of new vessels; acute regression of existing tumor vasculature can also be induced.

VEGF-A binding to VEGFR-2 drives receptor dimerization and trans-phosphorylation on key tyrosine residues, initiating downstream cytoplasmic signaling. A combination of biochemical and mass spectrometry analysis showed that the tyrosine residues Y951, Y1054,

Received 2/28/07; revised 5/25/07; accepted 6/27/07.

The costs of publication of this article were defrayed in part by the payment of page charges. This article must therefore be hereby marked *advertisement* in accordance with 18 U.S.C. Section 1734 solely to indicate this fact.

Requests for reprints: Simon T. Barry, Cancer and Infection Research, AstraZeneca, Mereside, Alderley Park, Macclesfield, Cheshire SK10 4TG, United Kingdom. Phone: 44-1625-513350; Fax: 44-1625-513624. E-mail: Simon.T.Barry@astrazeneca.com

doi:10.1158/1535-7163.MCT-07-0142

Y1059, Y1175, and Y1214 (of human VEGFR-2) are phosphorylated *in vitro* (9). Although these residues are important *in vitro*, it is unclear which sites are phosphorylated abundantly under physiologic or pathologic conditions in whole organisms. Phosphorylation at Y1175 is thought to result in the activation of the phospholipase Cγ and phosphoinositide-3-kinase pathways (10–12) and phosphorylated Y1214 thought to activate p38 mitogen-activated protein kinase signaling and regulate actin organization and possibly vascular permeability (3). More recently, phosphorylation at Y951 has been shown to couple a factor, termed T cell–specific adaptor, which activates src and modulates cell migration and vascular permeability (9).

AZD2171 is a potent small-molecule inhibitor of all three VEGFRs and VEGF-induced signaling in endothelial cells (6). It inhibits VEGFR-1, VEGFR-2, and VEGFR-3 recombinant kinases with IC_{50} values of 5, <1, and ≤3 nmol/L, respectively, and VEGFR-2 phosphorylation in human umbilical vascular endothelial cells (HUVEC) with an IC_{50} of 0.5 nmol/L. In addition, AZD2171 (0.75-6 mg/kg/day) dose-dependently inhibits the growth of a wide range of tumor xenografts following continuous once-daily p.o. administration. AZD2171 is currently in phase II and phase II/III clinical trials for the treatment of solid tumors. Understanding the relationship between target inhibition and the effect on the vasculature is important in elucidating how VEGF signaling inhibitors work. However, studying relevant pharmacodynamic changes in the phosphorylation of VEGFR-2 (preclinically or clinically) is challenging because of the low abundance of the receptor and the level of phosphorylation. The high homology between tyrosine phosphorylation sites of related receptors of the VEGFR and platelet-derived growth factor receptor (PDGFR) family also causes significant issues with cross-reactivity in biochemical and histologic assays. Generating informative data therefore depends on identifying key phosphorylation sites on the receptor *in vivo* and characterizing the most specific antibody tools for the end point of choice.

In this study, we have looked at the early effects of AZD2171 on the vasculature within Calu-6 tumor xenografts and the pharmacodynamic effect of the drug on VEGFR-2 activation *in vivo*. Screening antibodies to different phosphoepitopes on VEGFR-2 has identified two residues, and corresponding antibodies, that can be used to report the phosphorylation status of VEGFR-2 *in vivo*. We show that AZD2171 is a very effective inhibitor of VEGFR-2 signaling modeled in normal murine lung tissue where there is no detectable consequence of VEGFR-2 inhibition. A single 6 mg/kg dose of AZD2171 inhibits VEGF-A–stimulated phosphorylation of VEGFR-2 in murine lung tissue for up to 24 h. Furthermore, we show that AZD2171 reduces pVEGFR-2–positive vascular structures in Calu-6 tumors, and that this precedes the loss of tumor vasculature. These data support the hypothesis that inhibitors of VEGFR-2 activation can cause a relatively acute regression of tumor vasculature that is dependent on VEGF signaling for survival.

Materials and Methods

Reagents

Custom rabbit polyclonal antibodies CB1764 and 469 were generated against a peptide corresponding to human VEGFR-2 phosphotyrosine 1214 (Cambridge Research Biochemicals). Other antibodies were obtained from commercial sources: rabbit polyclonals against human pY1214/1212 (PS1012, Calbiochem) and human pY1175/1173 of VEGFR-2 (PC462, Oncogene Research), respectively; rabbit monoclonal against human VEGFR-2 (55B11, Cell Signalling Technology); rabbit polyclonal against mouse VEGFR-2 (sc-504, Santa Cruz Biotechnology); goat polyclonal against mouse CD31 antibody (sc-1506, Santa Cruz Biotechnology); and mouse monoclonal raised to α-smooth muscle actin (α-SMA; A2547, Sigma). The free base of AZD2171 (4-[(4-fluoro-2-methyl-1*H*-indol-5-yl)oxy]-6-methoxy-7-(3-(pyrrolidin-1-yl)propoxy)quinazoline; molecular weight = 450.51) was used for all preclinical studies as described in Wedge et al. (6). AZD2171 was suspended in 1% (w/v) aqueous polysorbate 80 and given (0.1 mL/10 g of body weight) by once-daily oral gavage to mice. Recombinant $VEGF_{165}$ was generated as described previously (13).

Murine Lung VEGFR-2 Pharmacodynamic Assay

To assess the effects on VEGFR-2 phosphorylation in murine lung, AZD2171 (0.75-6 mg/kg) or vehicle was given to female immunocompetent or nude (*nu/nu* genotype) Alderley Park (Swiss derived) mice. A bolus dose of VEGF-A (20 μg per mouse; R&D Systems, Abingdon or AstraZeneca) was given i.v. 5 min before humane termination of animals at specified time points (2-36 h), whereupon lungs were removed and immediately snap frozen in liquid nitrogen.

Frozen mouse lungs were homogenized in ice-cold lysis buffer [20 mmol/L Tris (pH 7.5); 137 mmol/L NaCl; 10% glycerol; 1% NP40; 50 mmol/L NaF; 1 mmol/L Na_3VO_4; 1 protease inhibitor tablet/25 mL buffer (Boehringer Ingelheim Ltd.)], treated with 0.1% SDS, and cleared by centrifugation. A lysate sample (250 μg) was separated by SDS-PAGE under reducing conditions and transferred to a nitrocellulose membrane (Invitrogen Ltd.) by Western blotting. Membranes were blocked in TBS containing 0.05% Tween (TBST) and 5% nonfat dry milk (Marvel) or 5% bovine serum albumin (BSA; Sigma-Aldrich Co., Ltd.) for 1 h at room temperature followed by an overnight incubation at 4°C in TBST (TBS and 0.5% Tween) with either Marvel or BSA. After washing, immunoblots were incubated with a horseradish peroxidase (HRP)–conjugated antirabbit antibody (New England Biolabs [NEB] Ltd.), HRP-conjugated antimouse antibody (NEB) or HRP-conjugated antigoat antibody (DAKO Ltd.). Immunoreactive bands were visualized using the Supersignal West Pico Substrate or Supersignal West Femto Substrate method of detection (Perbio Science UK Ltd.).

Tumor Studies

Protocols for establishing Calu-6 human lung tumor xenografts in female nude mice were as described previously (13). When tumors reached a volume of 1 cm^3,

mice were randomized (six per group) and dosed once daily by oral gavage with AZD2171 (6 mg/kg) or vehicle. Tumors were collected (six per group) 4 h after the last dose of AZD2171 or vehicle, on days 1 (4 h), 2 (28 h), and 3 (52 h), and fixed in formalin for 24 h before being embedded in paraffin.

Immunohistochemistry and Immunofluorescence

Formalin-fixed paraffin-embedded tumors from each study group were sectioned at 4 μm, dewaxed, and rehydrated. Antigen retrieval was done in DAKO buffer S1699, for all antibodies except total VEGFR-2 antibody (55B11), where DAKO buffer S3307 was employed. Antigen retrieval was done at 121°C for one cycle in a 2100-retriever pressure cooker (R2100-UK, PickCell Laboratories). All incubations were done at room temperature, and all washes were done with TBST. Endogenous biotin was blocked with avidin-biotin block (X0590, DAKO). For CD31, sections were blocked with 5% rabbit serum (DAKO) in TBST for 20 min and then incubated in a 1:50 dilution of CD31 antibody (sc-1506) in serum block for 1 h before washing. Biotinylated rabbit anti-goat immunoglobulin (DAKO), diluted 1:200, was then added to the sections for 30 min. For pVEGFR-2 and tVEGFR-2, sections were blocked with 5% goat serum (DAKO) in TBST for 20 min and then incubated with either a 1:50 dilution of pVEGFR-2 antibody (CB1764) or 1:40 dilution of tVEGFR-2 antibody (55B11) in serum block for 1 h. After washing a 1:200 dilution of biotinylated goat anti-rabbit immunoglobulin (DAKO) was added for 30 min. For all antibodies, Vectastain ABC-Elite solution, diluted as instructed in kit, was then added for 30 min, and the sections were developed in diaminobenzidine for 10 min (Biogenex) and counterstained weakly with Carazzi's hematoxylin. Routine controls used were no primary antibody and immunoglobulin G (IgG) instead of primary antibody. To control for recognition of phosphoepitopes, sections were pretreated with calf intestinal phosphatase (NEB), 200 units per mL in 1× NEB buffer 3 for 1 h at 37°C before the addition of primary antibody.

For all immunofluorescence on formalin-fixed tissues, antigen retrieval was done as above, and then sections were blocked in 20% horse serum in TBST for 20 min. Sections were incubated with either sc-1506 (1:50), PC462 (1:100), or CB1764 (1:100) in serum for 1 h, washed, and then incubated in the dark for 30 min with 1:50 donkey anti-goat IgG conjugated to Alexa Fluor 488 for CD31 (A11055, Molecular Probes) or 1:50 donkey anti-rabbit IgG conjugated to Alexa Fluor 488 (A21206, Molecular Probes) for pVEGFR-2. Double-staining experiments were done using pVEGFR-2/CD31 and pVEGFR-2/α-SMA (A2547) antibody combinations at 1:100/1:50 and 1:100/1:1,000, respectively. Appropriate secondary antibody pairs were combined at 1:50 in horse serum; pVEGFR-2 was detected with Alexa Fluor 488 secondary as above, CD31 and α-SMA were detected with donkey anti-goat IgG conjugated to Alexa Fluor 594 (A11058, Molecular Probes) and donkey anti-mouse IgG conjugated to Alexa-Fluor 594 (A21203, Molecular Probes). All fluorescently stained sections were counterstained using ProLong Gold antifade reagent with 4′,6-diamidino-2-phenylindole (DAPI; P36931, Molecular Probes), visualized using an Axiovert S100 fluorescent microscope (Carl Zeiss SMT Inc.) and images captured using MetaMorph version 6.1 software (Universal Imaging Co.).

Regional Analysis of MVD

The regional effects of AZD2171 on MVD at the periphery of xenografts compared with their core were quantified as follows. MVD analysis was done blinded using an Automated Cellular Imaging System (ACIS, ChromaVision Medical Systems Inc.). Briefly, each tissue section was scanned into the ACIS at ×10 magnification. Using the ACIS MVD software algorithm, an analysis threshold was set and applied to all tumors within the study. The viable tumor area at the periphery (~500 μmol/L in from the tumor edge) and core (~500 μmol/L out from the necrotic core) within each section was then selected for MVD analysis. MVD for each tumor was expressed as the mean number of CD31-positive vascular structures per square millimeter of viable tumor.

pVEGFR-2:CD31 Analysis

The pVEGFR-2:CD31 ratio for each xenograft was measured using two approaches because of the differences in detecting end points using PC462 and CB1764. First, serial sections from each tumor were fluorescently immunostained for pVEGFR-2 (PC462) and CD31. The number of pVEGFR-2– and CD31-positive vascular structures were then counted at the periphery of the tumor (two fields of view in from the edge) using a ×40 objective on an Axiovert S100 fluorescent microscope. The pVEGFR-2:CD31 vascular ratio for each tumor rim was then calculated using the formula: total number of pVEGFR2-positive vascular structures/total number of CD31-positive vascular structures. In the second approach, serial sections were chromogen stained for pVEGFR-2 (CB1764) and CD31 and scanned into the ACIS (ChromaVision Medical Systems Inc.) at ×10 magnification and the ACIS MVD algorithm applied to each. Analysis thresholds were set for pVEGFR-2 and CD31 and applied to all samples viable tissue at the periphery of each tumor was selected and analyzed to generate the number of pVEGFR-2– or CD31-positive vessels structures per area analyzed. Finally, the pVEGFR-2/CD31 vascular ratio at the tumor periphery was calculated using the formula number of pVEGFR-2–positive vascular structures per square millimeter viable tumor/number of CD31-positive vascular structures per square millimeter viable tumor.

Statistical Analysis of MVD and pVEGFR-2 Changes by Immunohistochemistry

All CD31 MVD and pVEGFR-2 data were analyzed for significant differences between the mean values from groups of control and AZD2171-treated tumors. Due to the small group sizes, the analysis has been carried out nonparametrically using the Mann-Whitney *U* test for unmatched samples. These results are in accordance with results obtained using a parametric test (data not shown). Data within a group were summarized using a geometric mean and also as a 95% confidence interval (95% CI) for the geometric mean, constructed on the logged data, and then back-transformed onto the original scale.

Table 1. Evaluation of antibodies to pVEGFR-2

VEGFR2 phosphoepitope	Western blot analysis (HUVEC + VEGF-A ± AZD2171)	Immunohistochemistry (Calu-6 xenografts)
pY951 RP (CST-2471)	Positive (very weak)	Negative
pY966 RP (CST-2474)	Negative (cross-reactive)	Stains tumor vessels
pY1054 RP (Biosource 44-1046)	Positive (cross-reactive)	Positive but variable (additional tumor cell staining)
pY1054/59 RP (Biosource 44-1047)	Positive (cross-reactive)	Positive but variable (additional tumor cell staining)
pY1175/1173 RP (Oncogene Res PC462)	Positive (weak)	Positive (specific for tumor vasculature)
pY1214/1212 RP (CalbiochemPS1012)	Positive* (clean)	Negative
pY1214/1212 RP (AZ 469)	Positive (clean)	Negative
pY1214/1212 RP (AZ CB1764)	Positive (clean)	Positive (specific for tumor vasculature)

NOTE: Positive indicates for Western blot; antibody specifically recognizes pVEGFR-2; for immunohistochemistry, antibody recognizes phosphoepitope in tumor vasculature. Negative indicates for Western blot; antibody does not recognize pVEGFR-2; for immunohistochemistry, antibody does not bind tumor vasculature.
Abbreviations: RP, rabbit polyclonal; AZ, AstraZeneca.
*Batch specific.

Results

Identifying Antibodies that Recognize pVEGFR-2

AZD2171 has shown profound inhibition of tumor growth across a range of subcutaneous (6) and orthotopic (14, 15) human tumor xenografts and in murine transgenic and spontaneous tumor models (16, 17). Although *in vitro* data indicate that AZD2171 is a highly potent inhibitor of VEGFR-2, direct inhibition of pVEGFR-2 *in vivo* has not been shown previously.

To identify antibody tools appropriate to assess VEGFR-2 phosphorylation in preclinical tissue, we screened a set of commercial antibodies as well as antibodies that we generated against pVEGFR-2. All antibodies were screened using Western blot analysis of HUVECs stimulated with VEGF-A in the presence and absence of 10 nmol/L AZD2171. Antibodies to phosphoepitopes were scored positive in the Western blot analysis if they recognized pVEGFR-2 in cell lysates of cells stimulated with VEGF-A and not in cells treated with AZD2171 (Table 1). This approach identified antibodies recognizing the phosphotyrosine residues pY1054, pY1059, pY1175, and pY1214 on VEGFR-2 (summarized in Table 1). Treatment of HUVECs with VEGF-A only resulted in weak phosphorylation of pY951 (data not shown). Interestingly, phosphorylation of VEGFR-2 was not detectable with an antibody to pY996. Although antibodies against the phosphotyrosine residues pY1054 and pY1059 recognized pVEGFR-2 by Western blot analysis, they also showed significant cross-reactivity with other phosphoproteins under the conditions used (indicated in Table 1). Although a number of monoclonal antibodies against a variety of phosphoepitopes were screened, none met our validation criteria, probably due to sensitivity. The positive antibodies were also screened for specific binding to Calu-6 tumor vasculature of xenografts by immunohistochemistry (summarized in Table 1). Although a number of antibodies recognized vessels, not all antibodies detected vessels by immunohistochemistry and pVEGFR-2 by Western blotting. For example, vascular staining was observed with the antibody to pY996, despite the fact that it did not recognize pVEGFR-2 in VEGF-A–stimulated HUVEC lysates. Based on Western blot analysis and immunohistochemical screening, we focused on antibodies recognizing the phosphotyrosine residues pY1214 (CB1764 and PS1012) and pY1175 (PC462) for further studies. Antibodies to these epitopes specifically recognized pVEGFR-2 in HUVEC lysates with minimal cross-reactivity with other proteins and showed discrete staining of tumor vasculature in tumor xenograft tissue. When used to examine the activated recombinant kinase domains of the VEGFRs by Western blot analysis (data not shown), none of the three antibodies recognized pVEGFR-1 or pVEGFR-3. To further define selectivity, these antibodies were screened against cell lines expressing phosphorylated forms of the receptors c-Kit, Flt-3, PDGFRα, PDGFRβ, and CSF1-R. The three antibodies show minimal cross-reactivity with these receptors and other proteins within the lysates (data not shown).

AZD2171 Inhibits VEGF-A–Driven Phosphorylation of Tyrosine Residues pY1175 and pY1214 on VEGFR-2 in Murine Lung Tissue

Assessing changes in VEGFR-2 activation *in vivo* is difficult because VEGFR-2 is primarily expressed on endothelial cells that represent only a very small fraction of most tissues. However, comparatively high expression of VEGFR-2 is evident in murine lung, presumably because this is a well-vascularized tissue. We therefore used normal mouse lung tissue from animals treated with a 20-μg bolus of VEGF-A for 5 min before humane termination, and measured phosphorylation of VEGFR-2, with and without AZD2171 treatment, using methodology described previously (18). pVEGFR2 can be detected in murine lungs in the absence of VEGF-A stimulation; however, the levels showed significant variation between individual animals. Therefore, for the purposes of these experiments, we have used VEGF-A treatment to normalize the signal, reducing the variation within each group of animals and also the group sizes. The modulation of pVEGFR-2 in murine lung lysate was analyzed by Western blotting using the antibodies identified to pY1214/1212 (CB1764 and PS1012) and pY1175/1173 (PC462). pVEGFR-2 was readily detected in

the lungs of animals treated with VEGF-A (Fig. 1). Following a single dose of AZD2171 (6 mg/kg), phosphorylation of VEGFR-2 induced by VEGF-A was inhibited maximally 2 h after treatment. All three antibodies showed similar results in a number of experiments and exhibited minimal cross-reactivity with other proteins.

The dose dependency and kinetics of VEGFR-2 inhibition by AZD2171 were assessed in more detail (Fig. 2). The phosphorylation status of VEGFR-2 was determined 2 h after treatment with a single dose of AZD2171 (0.75, 1.5, 3 and 6 mg/kg; Fig. 2A and B). Nearly complete inhibition of VEGFR-2 phosphorylation was achieved with 6, 3, and 1.5 mg/kg, and phosphorylation was reduced by 52% following treatment with 0.75 mg/kg of AZD2171. The time course of VEGFR-2 inhibition following a single 6 mg/kg dose of AZD2171 was also examined (Fig. 2C and D). At this dose, VEGFR-2 phosphorylation was suppressed for up to 24 h and returned to control levels by 36 h. Collectively, these data show that AZD2171 is a potent inhibitor of VEGFR-2 phosphorylation *in vivo*, which is consistent with the antitumor effects seen with this compound in a broad range of tumor models.

Antibodies to pVEGFR-2 Residues pY1214/1212 and pY1175/1173 Stain Tumor Vasculature in Calu-6 Tumor Xenografts

Assessing the inhibition of VEGFR-2 phosphorylation in normal mouse lung offers an excellent surrogate model system to study the pharmacodynamic effect of AZD2171, but does not necessarily predict the effect of treatment on tumor vasculature. To understand the relationship between inhibition of VEGFR-2 phosphorylation and changes in MVD, we further validated the antibodies that had shown vessel-specific staining on tumor xenograft tissue sections. Identifying phosphospecific antibodies to pVEGFR-2 that are suitable for immunohistochemistry using formalin-fixed tissue has proven challenging with many antibodies cross-reacting with phosphoproteins other than pVEGFR-2.

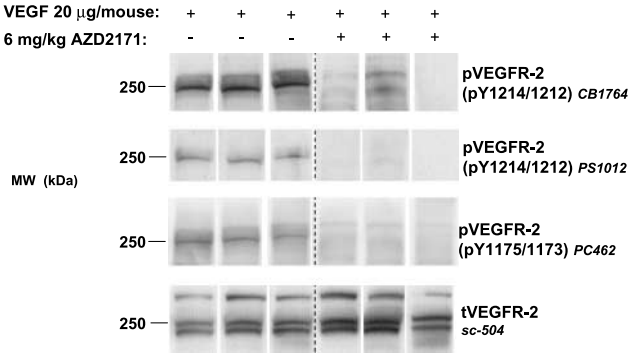

Figure 1. Validation of phosphospecific VEGFR-2 antibodies. Mice treated with one dose of AZD2171 (6 mg/kg) for 16 h and control mice (n = 3 per group) were given an i.v. bolus of VEGF-A for 5 min before sacrifice; the lungs were excised, homogenized, and analyzed by Western blotting using antibodies to VEGFR-2 (t, total; p, phosphorylated receptor) as indicated. Data shown are representative of two independent experiments.

CB1764 (pY1214/1212) and PC462 (pY1175/1173) showed vessel-specific staining in Calu-6 xenograft tissue with minimal staining of other cell types such as tumor cells (Fig. 3A and C, respectively). Davis et al. (5, 19) have shown previously that PC462 stains vasculature on frozen tissue, and our data show that this antibody can also be used on formalin-fixed tissue, with the best results obtained using a fluorescence-based end point. In addition, our data show that antibodies to pY1214/1212 on VEGFR-2 can be used to study modulation of receptor activation on tumor vasculature.

To confirm that both antibodies were specific for a phosphoepitope on tumor vasculature, a range of control experiments were done using tissue from Calu-6 human tumor xenografts (Fig. 3). Consistent with both antibodies binding to a phosphoepitope, neither antibodies stained vasculature in tumor sections pretreated with alkaline phosphatase (Fig. 3B and D). For cell type specificity, endothelial and supporting stromal cells were distinguished by staining with antibodies to CD31 and α-SMA (visualizing pericytes, smooth muscle, and/or fibroblast-like cells), respectively (Fig. 3E). Staining with an antibody to total VEGFR-2 showed that detectable expression of VEGFR-2 was restricted to vasculature (Fig. 3F). It is very unlikely that VEGFR-2 is expressed in other regions of Calu-6 tumors because the antibody used recognized both human and murine VEGFR-2 (data not shown). To ensure that the pVEGFR-2 antibodies were staining vasculature and not cells associated with vessels, sections were costained for either pVEGFR-2 and CD31 (Fig. 3G and I) or for pVEGFR-2 and α-SMA (Fig. 3H and J). Both phosphospecific VEGFR-2 antibodies showed coincident staining with endothelial cells (yellow overlay indicated by arrow; Fig. 3G and I), but not pericytes (Fig. 3H and J), consistent with the expression of total VEGFR-2. Taken together, these data indicate that both CB1764 and PC462 bind phosphoepitopes on VEGFR-2 expressed on endothelial cells and do not bind other stromal cells closely associated with the vessels. Moreover, the restricted staining pattern suggests that the antibodies have minimal cross-reactivity with other phosphoproteins.

AZD2171-induced Vessel Pruning Is Most Prominent toward the Tumor Periphery of Calu-6 Tumor Xenografts

Although chronic treatment with the majority of VEGF signaling inhibitors results in reductions in MVD, the effects of acute treatment of tumors are less clear. To understand the sequence of effects that AZD2171 has on tumor vasculature, changes in CD31-positive vessels were assessed in Calu-6 xenografts (1 cm^3) treated with one, two, and three doses of AZD2171 (4, 28, and 52 h postdosing, respectively) relative to time-matched control tumors.

We have shown previously that AZD2171 at 6 mg/kg/day induced a detectable change in the vasculature within viable regions of small tumors (0.2-0.4 cm^3) by 52 h (three doses), with this effect becoming more pronounced upon chronic treatment (6). To understand in more detail how acute treatment with AZD2171 impacts on tumor

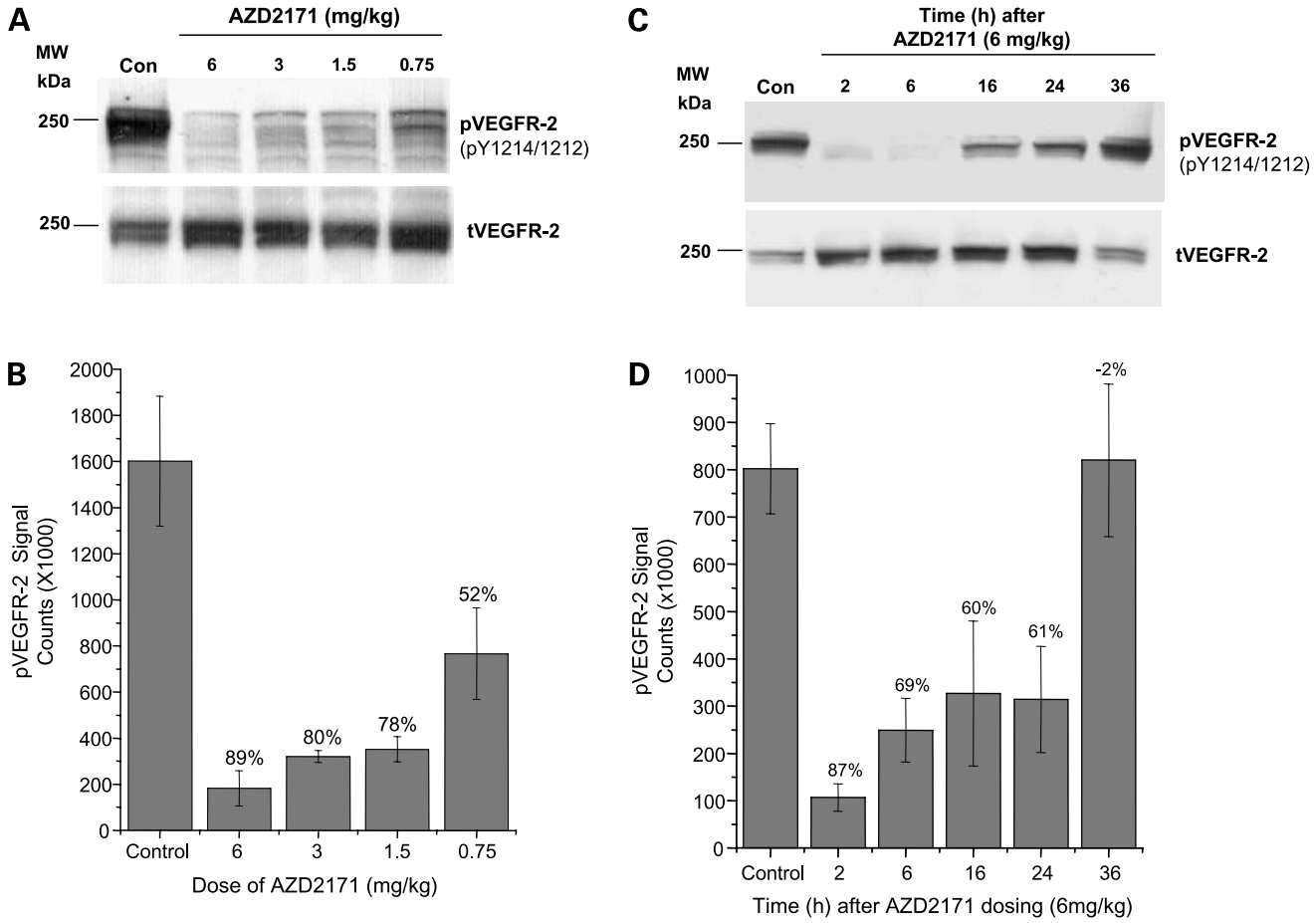

Figure 2. AZD2171 inhibits VEGFR-2 phosphorylation in murine lung tissue. Mice were treated with AZD2171 at doses ranging from 0.75 to 6 mg/kg as indicated ($n = 3$ per group). VEGF-A was given i.v. 5 min before sacrifice 2 h (**A, B**) or 2 to 36 h after AZD2171 administration (**C, D**). Lung homogenates were analyzed by Western blotting for pVEGFR-2 (pY1214/1212, CB1764) and VEGFR-2 as indicated. Western blots show data from one representative animal from each group (**A, C**); pVEGFR-2 signals from each group were quantitated by densitometry; the means ± SD are represented as percentage of the untreated control (**B, D**). Data are representative of two independent experiments.

vasculature in Calu-6 xenografts, we assessed the regional effects on vasculature, focusing on the periphery and core of the tumor. MVD analysis was done on all viable regions at the periphery and core of each tumor (shown schematically in Fig. 4A). The periphery of the tumor was defined as two-field widths at ×40 magnification or ~500 μm from the edge of the tumor, whereas the viable core was defined as two-field widths or ~500 μm from the necrotic core of the tumor. In control tumors, the MVD at the xenograft edge was approximately twice that of the core. AZD2171-induced changes were more pronounced at the rim of the tumors (Fig. 4B), with statistically significant changes in MVD occurring within 52 h (three doses) of compound administration and changes in MVD less apparent at 28 h.

AZD2171 Targets pVEGFR-2–positive Vessels within the Tumor Vascular Bed

Assessing the modulation in pVEGFR-2 levels within tumor vasculature by AZD2171 over time is challenging because of dynamic changes in tumor size and vascular content as a result of treatment. For the purpose of the current study, we examined the acute effects of AZD2171 in large (1 cm^3) human Calu-6 tumor xenografts. Given that the periphery of the tumor had the highest MVD and showed the greatest change in response to AZD2171, we focused on this region of the tumor to assess pVEGFR-2 modulation by AZD2171 over time. Because the first two doses (4 and 28 h) of AZD2171 induced only minimal changes in MVD, the 4-, 28-, and 52-h time points were most appropriate to examine changes in pVEGFR-2 status. Performing the pVEGFR-2 analysis at these early time points minimizes the variation in the data caused by vascular pruning and by differences in the size of the tumors.

The distribution of pVEGFR-2 was examined using antibodies to both pY1214/1212 (CB1764) and pY1175/1173 (PC462). The methods used to quantify staining with each antibody differed slightly because of the end points used for detection (CB1764 by chromagen and PC462 by fluorescence). Structures staining positive for pY1214/1212

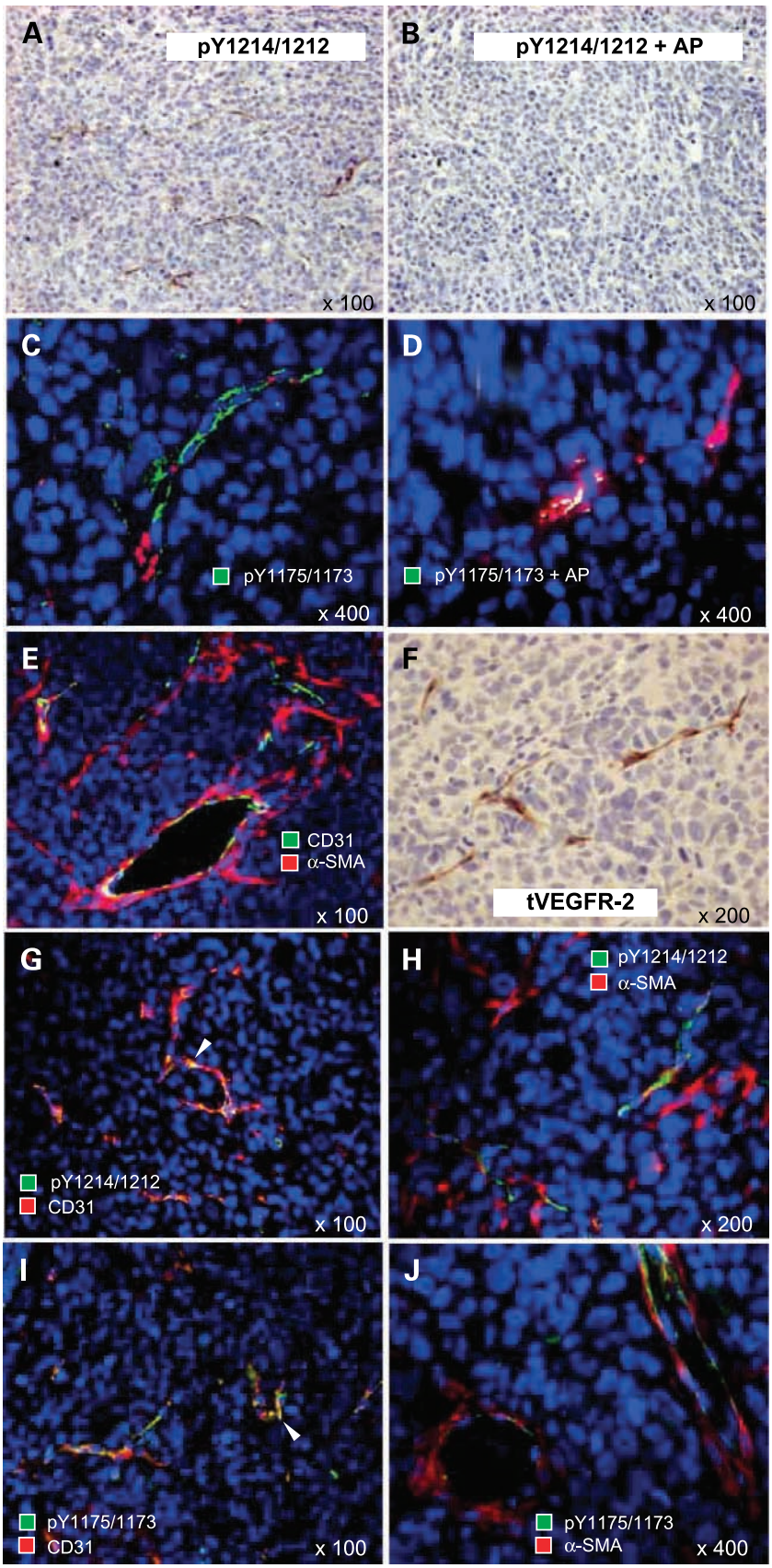

Figure 3. Validation of VEGFR-2 antibodies for immunohistochemistry. Vessel-specific staining for phosphospecific VEGFR-2 antibodies, CB1764 (pY1214/1212; **A**) and PC462 (pY1175/1173; **C**) and total VEGFR-2 antibody, 55B11 (**F**) using chromogen (**A, F**), and fluorescent (**C**) end points were shown on formalin-fixed Calu-6 tumor xenograft sections. Cell nuclei were visualized by counterstaining with DAPI (*blue*), and autofluorescing RBC within vessels are also evident (*red*; **C**). Phosphatase treatment of sections removed all phospho – VEGFR-2 – specific staining with CB1764 (**B**) and PC462 (**D**). To distinguish endothelial cells from supporting stromal cells, sections were costained for CD31 (endothelial cells) and α-SMA (supporting stromal cells; **E**). Endothelial cell-specific pVEGFR2 staining was shown by double immunofluorescence using pVEGFR2 antibodies (as above) and vessel markers, CD31 (**G, I**; colocalization indicated by arrow heads) and α-SMA (**H, J**). Images were taken from regions with high α-SMA positivity.

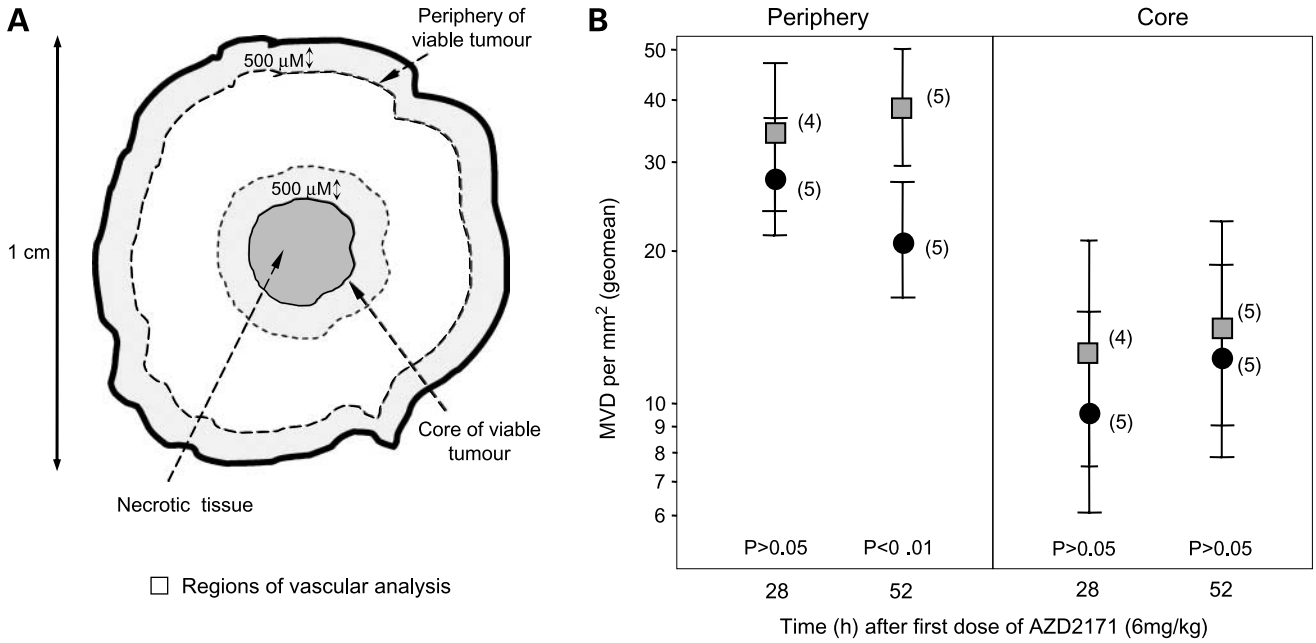

Figure 4. Regional effect of AZD2171 on Calu-6 lung tumor xenografts. **A,** schematic depicting a cross-section of a tumor xenograft. **B,** regional analysis of MVD. Tumor sections from AZD2171-treated (*circles*) and vehicle control (*squares*) groups were stained for CD31 ($n \geq 3$ per group). Using an ACIS at ×10 magnification, the mean vessel number per square millimeter of viable tumor (MVD) at the periphery and the core of each tumor was assessed. The geometric mean of each data point is represented together with the 95% CI for that value. The statistical significance for each time-matched data point was calculated using the Mann-Whitney *U* test, and the *P* value is represented. The numbers of tumors analyzed in each group are indicated in brackets adjacent to each data point.

(CB1764) and CD31 were counted using a ChromaVision ACIS. In contrast, structures stained for pY1175/1173 (PC462) and CD31-positive vascular structures were counted by eye. For both methods of quantification, single endothelial cells, endothelial cell clusters, immature vessels, and mature vessels staining for either pVEGFR-2 or CD31 were classified as positive vascular structures, and each were given a score of 1. The number of pVEGFR-2–positive structures in the periphery of the tumor was determined (Fig. 5A) and also expressed relative to the number of CD31-positive structures (Fig. 5B).

As shown in Fig. 5A, pVEGFR-2–positive structures (pY1175/1173 and pY1214/1212) are significantly reduced after treatment with AZD2171 for 28 h (two doses), with the effect maintained at 52 h (three doses) when vessel regression became evident (Fig. 4B). The effect was less obvious at 4 h. When the number of pVEGFR-2–positive structures is expressed relative to the CD31-positive structures, the data show that pVEGFR-2 staining was reduced at both the 28- and 52-h time points (Fig. 5B). From this method of analysis, it is not clear to what extent pVEGFR-2 was affected by AZD2171 at 4 h; the difference between control and treated tumors was not significant for either the pY1175/1173 or pY1214/1212 epitopes. Collectively, these data clearly show that AZD2171 reduces the number of pVEGFR-2–positive vascular structures, which subsequently results in a reduction in the number of microvessels within the periphery of the tumor.

Discussion

Being able to monitor changes in phosphorylation of VEGFR-2 *in vivo* is important if we are to understand the relationship between target inhibition and onset of effects within a tissue. However, deriving proof of mechanism for agents that target VEGFR-2 signaling has been challenging because of the low abundance of the target, limitations (specificity and sensitivity) of many of the available antibodies generated to pVEGFR-2, and knowledge of the major phosphoepitopes present on VEGFR-2 *in vivo*. We therefore characterized a series of antibodies for their suitability to detect the pharmacodynamic effect of AZD2171 on VEGFR-2 activation *in vivo*. Understanding the specificity and sensitivity of each purified polyclonal antibody preparation was key; as an example, from 15 polyclonal antibody preparations generated to pY1214/1212, only CB1764 met our validation criteria for use in immunohistochemistry.

Recent *in vitro* data suggest that only certain potential tyrosine phosphorylation sites on VEGFR-2 are phosphorylated in human endothelial cells in culture, namely, Y951, Y1054/59, Y1175, and Y1214 (9). Consistent with this finding, we found that phosphospecific antibodies to Y951, Y1054/59, Y1175, and Y1214 recognized pVEGFR-2 in HUVEC lysates, although pY951 was not detected as readily as other sites. A major issue associated with the use of phosphospecific antibodies is the potential for cross-reactivity with other receptors from the same kinase family. For antibodies to pVEGFR-2, this may include

cross-reactivity to other members of the VEGFR family, members of the related PDGFR family of kinases, or other phosphoepitopes. The antibodies to pY1175/1173 and pY1214/1212 specifically recognized pVEGFR-2 in murine lung lysates, showing minimal cross-reactivity with other phosphoproteins. In immunohistochemistry, these antibodies specifically stained tumor vasculature in Calu-6 tumors, with minimal cross-reactivity to other cell types within the tumor. These epitopes seem most specific to VEGFR-2. Although it is possible that these antibodies may bind the most closely related epitopes VEGFR-1 and VEGFR-3 under certain conditions, we saw no evidence of cross-reactivity within our *in vitro* or *in vivo* analyses. Although *in vitro* analyses show some minimal cross-reactivity with members of the PDGFR family phosphoproteins, we saw no evidence of cross-reactivity in our analysis of murine lung or xenograft tissue used in this study.

Although it is not clear which sites on VEGFR-2 are abundantly phosphorylated *in vivo*, our data suggest that phosphorylation at residues Y1175/1173 and Y1214/1212 can be detected robustly both in lung (by Western blotting) and in tumor vessels (by immunohistochemistry). The antibody to pY1214/1212 (CB1764) shows the most specific vessel staining with minimal background, reflecting either the affinity and specificity of the antibody or that this epitope is particularly accessible in tumor tissue. Assessing phosphorylation at residues Y1175/1173 and Y1214/1212 *in vivo* is relevant because they clearly play a role in

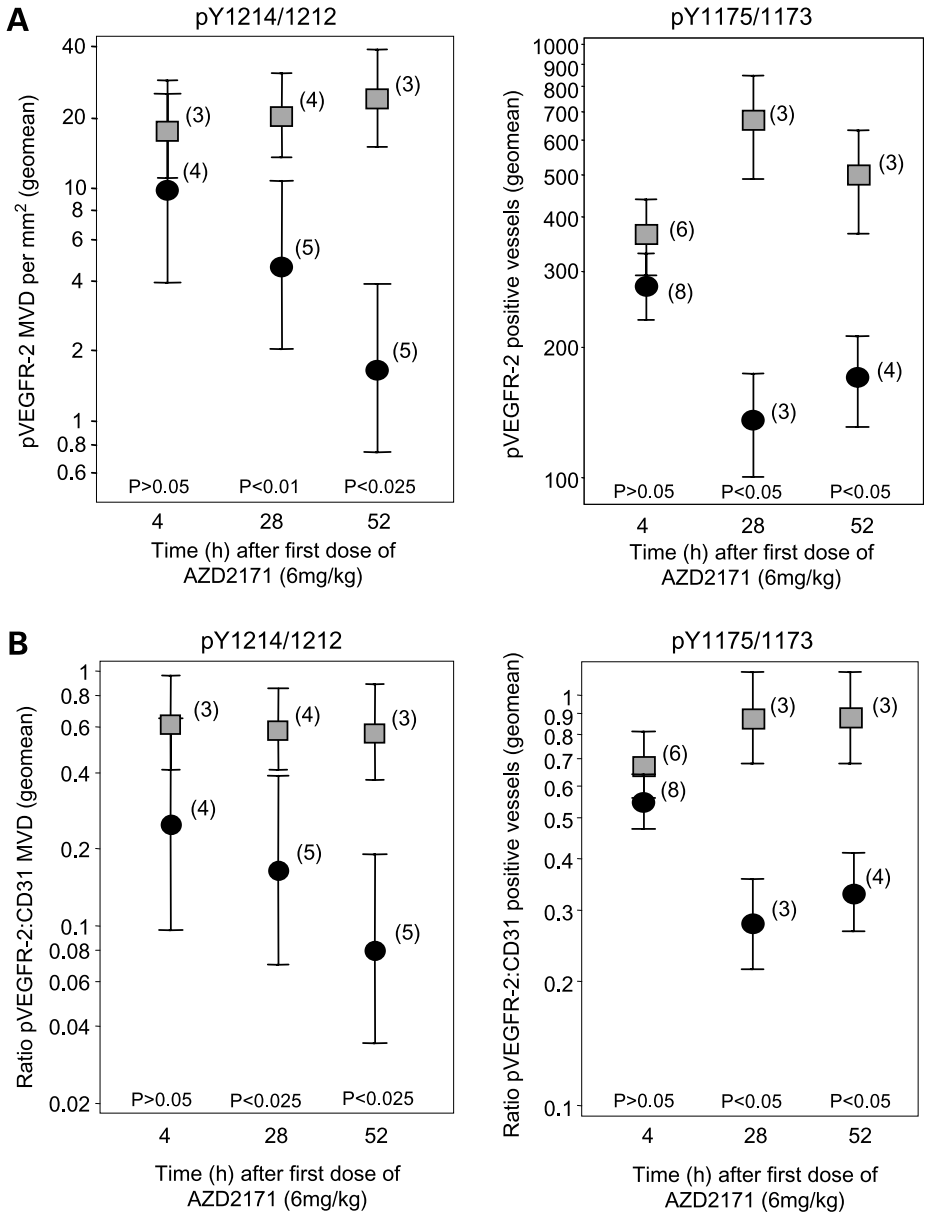

Figure 5. AZD2171 inhibits VEGFR-2 phosphorylation in tumor vasculature. Calu-6 tumor xenograft–bearing animals were treated with AZD2171 (6 mg/kg/day; *circles*) or vehicle (*squares*) for the times indicated ($n \geq 3$ per group). Serial sections from tumors were immunostained for pVEGFR-2 using CB1764 (pY1214/1212) and PC462 (pY1175/1173) antibodies, and vessels were visualized with an antibody to CD31. pVEGFR-2– and CD31-positive vessels in the periphery of the tumor were quantified using the ACIS for CB1764 (pY1214/1212) or counted manually within the entire tumor rim using a ×40 objective magnification for PC462 (pY1175/1173) (**A**). The ratio of p-VEGFR-2–positive structures to CD31-positive structures (MVD for pY1214/1212 and number of vessels for pY1175/1173) was calculated for each tumor (**B**). The geometric mean of each data point (MVD) is represented together with the 95% CI for that value (**A, B**). The statistical significance for each time-matched data point was calculated using the Mann-Whitney *U* test, and the *P* value was shown. The numbers of tumors analyzed in each group is indicated in brackets adjacent to each data point.

VEGFR-2 signaling. In particular, a somatic mutation of the Y1175/1173 site (in mouse) results in embryonic lethality (20). In contrast, although a mutation of Y1212 *in vivo* does not result in embryonic lethality (20), phosphorylation at Y1214/1212 is required for full activation of VEGFR-2–mediated signaling in endothelial cells and mediates key cellular responses such as actin remodeling, migration, and vascular permeability (10, 11, 21). More recently, modulation of phosphorylation of Y951 in preclinical tumor lysates by inhibitors of the VEGF signaling pathway has been reported (22). The failure to detect phosphorylation at residue Y951 probably reflects limitations in the sensitivity of the antibody and/or methodology used, rather than indicating that this residue is not phosphorylated because phosphorylation at this site is critical for pathologic angiogenesis (9).

The pharmacodynamic changes observed in murine lung tissue show that AZD2171 is a potent inhibitor of VEGFR-2 *in vivo*, consistent with the inhibition of VEGFR-2 phosphorylation shown previously *in vitro* (6). A single oral dose of AZD2171 can cause effective and prolonged inhibition of VEGF-A–induced VEGFR-2 phosphorylation over a 24-h period, consistent with once-daily dosing being sufficient to produce highly significant effects on tumor vasculature and growth. Interestingly, the levels of total VEGFR-2 seem to increase in lung lysates from animals dosed with AZD2171. At all doses, the increase mirrors the inhibitory effect of AZD2171 on receptor activation. After treatment with 6 mg/kg of AZD2171, the total VEGFR-2 levels return to control levels when VEGFR-2 is no longer inhibited by AZD2171 (36 h) and phosphorylation of the receptor is evident again. This increase in total VEGFR-2 is probably due to AZD2171 stabilizing the receptor, which would otherwise be internalized, recycled, or degraded upon activation. Similar effects have been seen in AZD2171-treated HUVECs *in vitro* (6). Total VEGFR-2 has also been reported to increase *in vivo* following chronic administration of DC101, an antibody to VEGFR-2, in 253J-BV bladder xenografts (5), which the authors suggest is linked to regional hypoxia, but could be enhanced as a result of receptor accumulation. Clearly, because the regulation of VEGFR-2 is a dynamic process, it will be interesting to understand how different classes of therapy affect receptor levels and recycling, temporally.

Acute responses to different VEGF signaling inhibitors have been studied in a variety of model systems, including xenograft and transgenic tumor models (4–8). Despite the diversity of model systems, vessel regression is commonly observed within 1 to 3 days of treatment. AZD2171 also caused acute vascular regression in tumor xenografts within a few days of treatment. Reductions in MVD have been observed previously after 52 h (three doses of AZD2171) in small (<0.4 cm^3) Calu-6 tumors (6). This current study further explored the nature of the vascular response to AZD2171 using large (1 cm^3) Calu-6 tumors by comparing regional responses to AZD2171 in the tumor periphery and core. A reduction in vessel density was only apparent in the periphery of the tumors at these early time points, indicating that in the rapidly growing rim of the tumor, a significant proportion of vessels are acutely sensitive to VEGFR-2 inhibition.

In addition to the acute effects observed on tumor vasculature, chronic treatment with AZD2171 for 2 weeks and longer at 6 mg/kg/day reduces vascular density within Calu-6 tumors by up to 75% (6). This suggests that VEGF signaling inhibitors are likely to induce two distinct responses within the tumor: an acute response that limits the growth of tumor xenografts by pruning a subset of sensitive vessels, and a chronic effect that prevents new vessel growth within the tumor and/or further prunes less sensitive vessels. This could have implications for the design of clinical trials as the relevant pharmacodynamic changes in VEGFR phosphorylation may need to be assessed after a limited number of doses with compound.

The magnitude of the acute vascular response in different tumor settings may possibly be dependent on the phenotype of the vessels within the tumor. Inai et al. (4) have shown inhibition of VEGF signaling to cause rapid regression of highly sensitive vessels, both within tumor tissue and normal fenestrated endothelium. In the transgenic RIP-Tag2 pancreatic islet tumor model, a rapid vascular regression is observed following treatment with both VEGF-Trap and AG013736 (4). The time of onset and extent of vessel regression seem more rapid than observed in Calu-6 tumors, suggesting that perhaps in the transgenic RIP-Tag2 model, a greater proportion of vessels have a higher dependency on VEGFR-2 signaling for survival.

To study the modulation of VEGFR-2 in tumor vasculature, we assessed the ratio of the number of structures staining positive for pVEGFR-2 and CD31. There is a clear reduction in the number of pVEGFR-2–positive structures after 28 h of treatment with AZD2171, which is maintained at 52 h. The change in pVEGFR-2 and the fraction of pVEGFR-2–positive vessels relative to the total number of vessels are statistically significant with antibodies to both phospho-sites on VEGFR-2, with a clear separation in the 95% CIs. When comparing the effects of AZD2171 on lung versus tumor vasculature, a difference in the level of pVEGFR-2 inhibition was following a single dose of AZD2171. Phosphorylation of VEGFR-2 in lung tissue was inhibited markedly, whereas its phosphorylation in tumor was not. It is not clear whether this reflects diverse ways in which VEGFR-2 phosphorylation is regulated in different tissues or differences in the sensitivity of the methods used. We attempted to directly compare VEGFR-2 modulation in both lung and tumor by Western blot analysis, but were unable to robustly detect pVEGFR-2 in Calu-6 tumor lysates presumably because of its comparative low abundance. The immunohistochemical analysis we have done does not take into account the intensity of staining but scores vessel structures either positive or negative for pVEGFR-2 and would therefore not distinguish structures in which the levels of pVEGFR-2 were reduced relative to controls. It is also possible that differences at this early time point may reflect either the relative rates of turnover of phosphorylation of VEGFR-2 in lung

and tumor tissue, or that it is harder to inhibit VEGFR-2 signaling in larger, well-established tumors with poor or heterogeneous blood flow. If the latter is relevant in the clinical setting, it will be key to have potent agents that can attain sustained plasma exposure, such as AZD2171, to achieve and maintain significant inhibition of VEGFR-2 signaling on tumor vasculature.

In summary, we have shown that acute treatment with AZD2171 prunes a subset of vessels in the periphery of the tumor, and that inhibition of VEGFR-2 phosphorylation precedes this change, consistent with the mode of action of AZD2171. These data confirm that AZD2171 is a potent inhibitor of VEGF signaling *in vivo*.

References

1. Ferrara N. Role of vascular endothelial growth factor in physiologic and pathologic angiogenesis: therapeutic implications. Semin Oncol 2002;29:10–4.

2. Olsson AK, Dimberg A, Kreuger J, Claesson-Welsh L. VEGF receptor signalling—in control of vascular function. Nat Rev Mol Cell Biol 2006;7:359–71.

3. Hurwitz H, Fehrenbacher L, Novotny W, et al. Bevacizumab plus irinotecan, fluorouracil, and leucovorin for metastatic colorectal cancer. N Engl J Med 2004;350:2335–42.

4. Inai T, Mancuso M, Hashizume H, et al. Inhibition of vascular endothelial growth factor (VEGF) signaling in cancer causes loss of endothelial fenestrations, regression of tumor vessels, and appearance of basement membrane ghosts. Am J Pathol 2004;165:35–52.

5. Davis DW, Inoue K, Dinney CP, Hicklin DJ, Abbruzzese JL, McConkey DJ. Regional effects of an antivascular endothelial growth factor receptor monoclonal antibody on receptor phosphorylation and apoptosis in human 253J B-V bladder cancer xenografts. Cancer Res 2004;64:4601–10.

6. Wedge SR, Kendrew J, Hennequin LF, et al. AZD2171: a highly potent, orally bioavailable, vascular endothelial growth factor receptor-2 tyrosine kinase inhibitor for the treatment of cancer. Cancer Res 2005;65:4389–400.

7. Tong RT, Boucher Y, Kozin SV, Winkler F, Hicklin DJ, Jain RK. Vascular normalization by vascular endothelial growth factor receptor 2 blockade induces a pressure gradient across the vasculature and improves drug penetration in tumors. Cancer Res 2004;64:3731–6.

8. Miller DW, Vosseler S, Mirancea N, et al. Rapid vessel regression, protease inhibition, and stromal normalization upon short-term vascular endothelial growth factor receptor 2 inhibition in skin carcinoma heterotransplants. Am J Pathol 2005;167:1389–403.

9. Matsumoto T, Bohman S, Dixelius J, et al. VEGF receptor-2 Y951 signaling and a role for the adapter molecule TSAd in tumor angiogenesis. EMBO J 2005;24:2342–53.

10. Holmqvist K, Cross MJ, Rolny C, et al. The adaptor protein shb binds to tyrosine 1175 in vascular endothelial growth factor (VEGF) receptor-2 and regulates VEGF-dependent cellular migration. J Biol Chem 2004;279:22267–75.

11. Takahashi T, Yamaguchi S, Chida K, Shibuya M. A single autophosphorylation site on KDR/Flk-1 is essential for VEGF-A–dependent activation of PLC-γ and DNA synthesis in vascular endothelial cells. EMBO J 2001;20:2768–78.

12. Dayanir V, Meyer RD, Lashkari K, Rahimi N. Identification of tyrosine residues in vascular endothelial growth factor receptor-2/FLK-1 involved in activation of phosphatidylinositol 3-kinase and cell proliferation. J Biol Chem 2001;276:17686–92.

13. Wedge SR, Ogilvie DJ, Dukes M, et al. ZD6474 inhibits vascular endothelial growth factor signaling, angiogenesis, and tumor growth following oral administration. Cancer Res 2002;62:4645–55.

14. Drevs J, Esser N, Wedge SR, Ryan AJ, Oglivie DJ, Marme D. Effect of AZD2171, a highly potent VEGF receptor tyrosine kinase inhibitor, on primary tumor growth, metastasis and vessel density in murine renal cell carcinoma. Proc Am Assoc Cancer Res 2004;45:1051.

15. Wu W, Fujitaka K, Mandal J, et al. AZD2171, an oral, highly potent VEGFR signaling inhibitor, in combination with gefitinib or paclitaxel: results of a study in an orthotopic human lung adenocarcinoma model. Clin Cancer Res 2005;11:B7.

16. Klinowska TC, Jackson JA, Farrington PM, et al. AZD2171, a highly potent inhibitor of VEGF receptor tyrosine kinase activity, inhibits the growth of spontaneous mammary tumors in the MMTV-neu transgenic mouse. Proc Am Assoc Cancer Res 2004;45:1048.

17. Goodlad RA, Ryan AJ, Wedge SR, et al. Inhibiting vascular endothelial growth factor receptor-2 signaling reduces tumor burden in the ApcMin/+ mouse model of early intestinal cancer. Carcinogenesis 2006;27:2133.

18. Sepp-Lorenzino L, Rands E, Mao X, et al. A novel orally bioavailable inhibitor of kinase insert domain-containing receptor induces antiangiogenic effects and prevents tumor growth *in vivo*. Cancer Res 2004;64:751–6.

19. Davis DW, Takamori R, Raut CP, et al. Pharmacodynamic analysis of target inhibition and endothelial cell death in tumors treated with the vascular endothelial growth factor receptor antagonists SU5416 or SU6668. Clin Cancer Res 2005;11:678–89.

20. Sakurai Y, Ohgimoto K, Kataoka Y, Yoshida N, Shibuya M. Essential role of Flk-1 (VEGF receptor 2) tyrosine residue 1173 in vasculogenesis in mice. Proc Natl Acad Sci U S A 2005;102:1076–81.

21. Meyer RD, Dayanir V, Majnoun F, Rahimi N. The presence of a single tyrosine residue at the carboxyl domain of vascular endothelial growth factor receptor-2/FLK-1 regulates its autophosphorylation and activation of signaling molecules. J Biol Chem 2002;277:27081–7.

22. Casanovas O, Hicklin DJ, Bergers G, Hanahan D. Drug resistance by evasion of antiangiogenic targeting of VEGF signaling in late-stage pancreatic islet tumors. Cancer Cell 2005;8:299–309.

Molecular Cancer Therapeutics

Acute pharmacodynamic and antivascular effects of the vascular endothelial growth factor signaling inhibitor AZD2171 in Calu-6 human lung tumor xenografts

Neil R. Smith, Neil H. James, Ian Oakley, et al.

Mol Cancer Ther 2007;6:2198-2208.